Hindawi
International Journal of Aerospace Engineering
Volume 2020, Article ID 1764510, 12 pages
https://doi.org/10.1155/2020/1764510

Research Article

Discrete-Time Angle Constraint Interception with Model-Assisted Target Maneuver Estimator

Y. I. Sheng,[1] W. A. N. G. Jiang,[2,3] Pei Pei,[2,3] and Zhou Yongjia[4]

[1]*School of Mechatronical Engineering, Beijing Institute of Technology, Beijing 100081, China*
[2]*School of Aerospace Engineering, Beijing Institute of Technology, Beijing 100081, China*
[3]*Beijing Key laboratory of UAV Autonomous Control, Beijing Institute of Technology, Beijing 100081, China*
[4]*Northwest Industries Group CO., LTD, Xian, 710000, China*

Correspondence should be addressed to W. A. N. G. Jiang; wjbest2003@163.com

Received 6 March 2019; Revised 1 February 2020; Accepted 24 February 2020; Published 5 August 2020

Academic Editor: Maj D. Mirmirani

This paper investigates the problem of designing angle constraint guidance law against unknown maneuvering targets based on discrete-time sliding mode control theory. Invoking the fact that the future course of action of the target, an independent entity, cannot be predicted beforehand due to its complexity and unpredictability, a model-assisted discrete-time disturbance observer in cooperation with a singularity-free strategy is proposed first to estimate the target maneuver. Based on the reconstructed signal and a fast convergence time-varying sliding surface, a new chattering-mitigated super-twisting-like discrete-time impact angle constraint guidance law is then synthesized. Stability analysis shows that the closed-loop system trajectory can be forced to enter into a small region around the sliding surface. Simulations and comparisons with classical discrete-time sliding mode guidance law validate the effectiveness of the proposed guidance law.

1. Introduction

Proportional navigation guidance (PNG) law has been widely used in missile guidance system in the past few decades due to its easy implementation and might suffice for many typical cases of applications [1]. The baseline concept of PNG lies in that it generates a latex command proportional to the line-of-sight (LOS) rate to nullify the LOS rate so as to guide a pursuer onto the collision triangle for target capture. However, during realistic engagement for intercepting maneuvering targets, the performance of PNG degrades drastically and the assumption for linearized collision triangle may be violated [1–4]. To the overall guidance performance, the most well-known extension of the PNG law is the augmented PNG (APNG) law, which augments a biased term to the original PNG formulation to counteract the effect of target maneuver [1]. Compared to PNG law, the APNG law reduces the required missile latex at the time of impact as well as the total required control effort throughout the homing engagement. But, unfortunately, an accurate target maneuver model is required to bring such an improvement for APNG law, which greatly limits the application of APNG.

During the development of modern guidance law, the concept of imposing hard constraint on intercept angle or impact angle provides engineers a new view to design guidance laws for tactical missiles to exploit the weak points of the target and increase the overall kill probability [5–9]. In the literature, a considerable number of efforts that address the problem of impact angle control are based on optimal control theory with small-angle assumption around the collision triangle [5–9]. The reason why used linearized kinematics for optimal guidance law design lies in the fact that analytically solving Hamilton-Jacobi-Bellman partial differential equation for nonlinear systems is usually intractable [10]. The small-angle assumption itself, however, is usually not valid when considering large intercept angles since the pursuer trajectory may greatly deviate from the desired collision triangle to cater for large impact angle constraint [9].

With the development of modern control theory, sliding mode control (SMC) methodology was widely accepted in

angle constraint guidance law design for intercepting maneuvering targets [11–23]. In SMC guidance law design, most of the existing works viewed target maneuver as an external disturbance with known upper bound and using discontinuous sign function to counteract it [11–14]. Usually, the maximum maneuverability of a predesignated target is chosen as this upper bound in real applications. However, due to the unpredictability and complicity of target maneuvers, highly conservative bound requires excessive control energy consumption and severe chattering phenomenon will be excited, while lower upper bound will result in guidance performance degradation and even system instability. To address this dilemma, some elegant solutions were reported by using estimation algorithms to reconstruct the target maneuver profile online and augmenting the estimated signal to obtain a so-called add-on controller [4, 16–23]. Unfortunately, all the above mentioned SMC guidance laws were designed for continuous-time guidance systems, while the real interceptor can only change its guidance command at sampling instants, the command cannot respond to the designed continuous-time controller. When applying continuous-time controller to discrete system, firstly, the system can hardly reach and maintain on the sliding surface due to the discrete form; secondly, the continuous stable system may be unstable, the stability theory of discrete system is different; finally, the discrete system will result in time delay, chattering phenomenon, and invariable control command during sampling time [24]. These are the reasons why designing guidance law in discrete-time manner is more desirable for practical interceptors. Some invariance properties of continuous-time sliding mode control are not held in discrete-time sliding mode control, such as the system cannot stay on the sliding surface but move about the sliding manifold [25]. Based on the sampled-date systems, the sliding mode controller needs to be reconstructed.

Motivated by the above analysis, this paper considers designing discrete-time SMC impact angle guidance law for unknown maneuvering target interception. A robust discrete-time guidance SMC guidance law with a time-delay observer was designed by Wang [26] for maneuvering target interception as well as actuator faults, but impact angle constraints were not taken into account. To the best of our knowledge, this may be the first time to address the problem of angle constraint interception within discrete-time control framework. Nonlinear numerical studies show that the proposed guidance law can achieve accurate interception with wide range of impact angles. The key features and contributions of this paper are summarized as follows.

(1) An exponentially stable model-assisted disturbance observer is proposed to estimate the target maneuver online. Different from the existing target maneuver estimators [4, 15–22], the proposed design method is naturally a discrete-time and singularity-free strategy

(2) A discrete-time time-varying sliding surface is designed to accelerate the convergence speed of the LOS angle tracking error

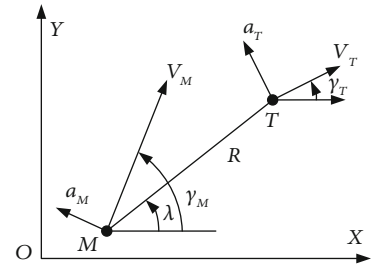

Figure 1: Planar homing engagement geometry.

(3) Based on the reconstructed target maneuver information, a new chattering-mitigated super-twisting-like discrete-time guidance law is proposed for accurate impact angle control. Theoretical analysis shows that the closed-loop system trajectory can converge into a small region around the designed sliding surface under the proposed guidance law

The rest of the paper is organized as follows. The problem formulation stated in Sec. II. In Sec. III, the proposed guidance law and convergence analysis are presented in details, followed by the simulation results provided in Sec. IV. Finally, some conclusions are offered in Sec. V.

2. Backgrounds and Preliminaries

In this section, engagement kinematics of maneuvering target interception with impact angle constraint is formulated for the analysis and the design of guidance law. The following general assumptions in guidance law design are considered for convenient analysis.

Assumption 1. (point mass interceptor and target). both the interceptor and the target are considered as point masses, e.g., only kinematics is considered in this paper.

Assumption 2. (ideal interceptor). the interceptor is considered as an ideal point mass such that the achieved acceleration is the same as the command signal generated by guidance law.

Assumption 3. (aerodynamically controlled interceptor). only aerodynamically controlled missiles are considered in this paper, which means that the missile acceleration along the LOS usually cannot be adjusted.

Assumption 4. (constant speed). both the interceptor and targets fly with constant speeds.

3. Model Derivation

Consider a typical two-dimensional engagement scenario shown in Figure 1, where the subscripts M and T denote the missile and the target, γ_M and γ_T the missile and the target flight path angle, λ and R the LOS angle and the missile-target relative range, V_M and V_T the missile and the target velocity, a_M and a_T the missile and the target

acceleration, which are normal to their corresponding velocities, respectively.

The corresponding equations describing the missile-target relative kinematics are formulated as

$$\dot{R} = V_T \cos(\gamma_T - \lambda) - V_M \cos(\gamma_M - \lambda), \tag{1}$$

$$\dot{\lambda} = \frac{1}{R}[V_T \sin(\gamma_T - \lambda) - V_M \sin(\gamma_M - \lambda)], \tag{2}$$

$$\dot{\gamma}_M = \frac{a_M}{V_M}, \tag{3}$$

$$\dot{\gamma}_T = \frac{a_T}{V_T}. \tag{4}$$

Let $V_r = \dot{R}$, $V_\lambda = R\dot{\lambda}$, differentiating Eqs. (1) and (2) with respect to time yields

$$\dot{V}_r = \frac{V_\lambda^2}{R} + a_{Tr} - a_{Mr}, \tag{5}$$

$$\dot{V}_\lambda = -\dot{R}\dot{\lambda} + a_{T\lambda} - a_{M\lambda}, \tag{6}$$

where $a_{Tr} = a_T \sin(\lambda - \gamma_T)$, $a_{Mr} = a_M \sin(\lambda - \gamma_M)$ represent the target and the missile accelerations along the LOS, respectively; $a_{T\lambda} = a_T \cos(\lambda - \gamma_T)$, $a_{M\lambda} = a_M \cos(\lambda - \gamma_M)$ denote the target and the missile accelerations normal to the LOS, respectively.

Compared with other variables, the relative range and its rate are slow-varying variables [1]. With this in mind and let T be the sampling period, a simple Euler discretization of Eqs. (5) and (6) at the kT time instant can be formulated as

$$\begin{aligned} V_r(k+1) - V_r(k) &= \frac{TV_\lambda^2(k)}{R(k)} + Ta_{Tr}(k) - Ta_{Mr}(k), \\ V_\lambda(k+1) - V_\lambda(k) &= -T\dot{R}(k)\dot{\lambda}(k) + Ta_{T\lambda}(k) - Ta_{M\lambda}(k). \end{aligned} \tag{7}$$

Assumption 5. The change rate of the target maneuver between two sampling intervals is bounded by a constant δ^*, i.e., $|\delta(k)| = |a_T(k+1) - a_T(k)| \le T\delta^*$. It should be noted that Assumption 5 is required in stability proof of the proposed disturbance observer. Actually, in real applications, the change rate of the acceleration of the target is very limited between two time sampling intervals due to physical limitations, and therefore, Assumption 5 is reasonable.

4. Guidance Strategy

To ensure successful target interception and kill probability, the pursuer should have to impose hard constraints on terminal miss distance as well as terminal impact angle. In this regard, the following two general definitions are introduced for the convenience of analysis.

Definition 1. (Zero-Effort-Miss-Distance) [27]. The term zero-effort miss, denoted by ZEM, at any time instant t is defined as the closest miss distance if both the pursuer and the target do not perform any maneuver from the time instant t onward. The definition of ZEM is [28].

$$ZEM(t) = \frac{rV_\lambda}{\sqrt{\dot{r}^2 + V_\lambda^2}}. \tag{8}$$

According to Eq. (8), one can conclude that zeroing V_λ leads to perfect interception with zero miss distance.

Definition 2. (Impact angle). The quantity impact angle, denoted as θ_{imp}, is defined as the angle between target velocity vector and pursuer velocity vector, i.e., $\theta_{imp} = \gamma_T - \gamma_M$.

Assuming a perfect interception is achieved, i.e., $V_\lambda = 0$, it follows from Eq. (2) that

$$V_T \sin(\gamma_T - \lambda) = V_M \sin(\gamma_M - \lambda). \tag{9}$$

Based on Eq. (9) and assume that the interceptor has advantageous velocity, e.g., $V_T/V_M < 1$, then one can imply that the impact angle and LOS angle have one-to-one correspondence, that is [12–14]

$$\lambda_F = \gamma_T - \tan^{-1}\left(\frac{\sin\theta_{imp}}{\cos\theta_{imp} - V_T/V_M}\right), \tag{10}$$

where λ_F denotes the desired LOS angle. It follows from Eq. (10) that the impact angle constraint can be satisfied by imposing a one-to-one correspondent LOS angle constraint. Considering this, the control interest here is to design a guidance law in such a way that the missile can capture the unknown maneuvering target with desired LOS angle λ_F.

5. Composite Guidance Law Design and Convergence Analysis

In this section, the proposed composite guidance law is derived in details, and the convergence analysis is also presented. A discrete-time model-assisted disturbance observer is firstly proposed to estimate the target maneuver. Then, a new discrete-time chattering-mitigated super-twisting-like guidance law is synthesized based on the designed sliding variable.

5.1. Disturbance Observer Design. Generally, by viewing the target maneuver as an external disturbance for the guidance system, classical disturbance observer can then be applied for target maneuver estimation, for instance, continuous time-delay estimator [4, 19], second-order sliding mode observer [20], inertial-delay control [21], higher-order sliding mode observer [17, 22], and extended state observer [18, 23]. Although the target maneuver can be estimated by these different types of observers, most of them are designed for continuous-time guidance laws. Different from these formulations, the proposed model-assisted observer is naturally based on discrete-time control approach, which is defined as

$$\hat{a}_{Tr}(k) = KV_r(k) - z(k), \tag{11}$$

$$z(k+1) = z(k) + K\left[\frac{TV_\lambda^2(k)}{R(k)} + T\hat{a}_{Tr}(k) - Ta_{Mr}(k)\right], \tag{12}$$

where $K > 0$ is an observer gain to be designed. Let $e(k) = a_{Tr}(k) - \hat{a}_{Tr}(k)$ be the disturbance estimation error, then one can obtain the error dynamics as

$$\begin{aligned} e(k+1) &= a_{Tr}(k+1) - \hat{a}_{Tr}(k+1) \\ &= a_{Tr}(k+1) - [KV_r(k+1) - z(k+1)] \\ &= a_{Tr}(k+1) - K\left[V_r(k) + \frac{TV_\lambda^2(k)}{R(k)} + Ta_{Tr}(k) - Ta_{Mr}(k)\right] \\ &\quad + z(k) + K\left[\frac{TV_\lambda^2(k)}{R(k)} + T\hat{a}_{Tr}(k) - Ta_{Mr}(k)\right] \\ &= a_{Tr}(k+1) - [KV_r(k) - z(k)] - KT[a_{Tr}(k) - \hat{a}_{Tr}(k)] \\ &= \underbrace{a_{Tr}(k+1) - a_{Tr}(k)}_{\vartheta(k)} + a_{Tr}(k) - \hat{a}_{Tr}(k) - KTe(k) \\ &= \vartheta(k) + \underbrace{(1 - KT)}_{M} e(k) = \vartheta(k) + Me(k), \end{aligned} \tag{13}$$

Theorem 1. *Consider error dynamics (13), if $|M| < 1$, then the estimation error can be bounded by*

$$\lim_{k\to\infty} |e(k)| \le \frac{\delta^* T}{1 - |M|}. \tag{14}$$

Proof. With error dynamics (13), one can imply that

$$|e(k+1)| = |\vartheta(k) + Me(k)| \le |\delta(k)| + |M||e(k)| \le \delta^* T + |M||e(k)|. \tag{15}$$

Solving inequality (15) gives

$$|e(k+1)| \le |M|^k e(0) + \delta^* T \sum_{i=1}^{k} |M|^i. \tag{16}$$

If the upper limit when k goes to infinity is considered, one can conclude that

$$\lim_{k\to\infty} |e(k)| \le \frac{\delta^* T}{1 - |M|}. \tag{17}$$

This completes the proof. It follows from Eq. (17) that the estimation error dynamics is exponentially stable with a small upper bound, and the bound can be lowered by increasing the observer gain K under the condition $|M| < 1$. If the rough value of target maneuver is known, one can initialize disturbance observer (12) with $z(0) = KV_r(0) - \tilde{a}_{Tr}(0)$, where $\tilde{a}_{Tr}(0)$ is the rough guess of target maneuver. From the practical point of view, however, it is better to initialize disturbance observer (12) with $z(0) = KV_\lambda(0)$ in terms of smoothing the transient control input, that is, from zero to a certain value to avoid the peaking phenomenon.

Similarly, the target maneuver perpendicular to the LOS can also be estimated via

$$\begin{aligned} \hat{a}_{T\lambda}(k) &= KV_\lambda(k) - \bar{z}(k), \\ \bar{z}(k+1) &= \bar{z}(k) + K\left[-T\dot{R}(k)\dot{\lambda}(k) + T\hat{a}_{T\lambda}(k) - Ta_{M\lambda}(k)\right]. \end{aligned} \tag{18}$$

With the above two target maneuver projection estimations, the real target maneuver estimation can be obtained by the following singularity-free strategy

$$\begin{aligned} \hat{a}_T(k) &= \sqrt{\hat{a}_{T\lambda}^2(k) + \hat{a}_{Tr}^2(k)}\ \text{sgn}\left[\hat{a}_{Tr}/\sin(\lambda - \gamma_T)\right] \ \text{or} \\ \hat{a}_T(k) &= \sqrt{\hat{a}_{T\lambda}^2(k) + \hat{a}_{Tr}^2(k)}\ \text{sgn}\left[\hat{a}_{T\lambda}/\cos(\lambda - \gamma_T)\right], \end{aligned} \tag{19}$$

where sgn $(\cdot)$ is the sign function. In [29], the authors used a simple strategy $\hat{a}_T(k) = \hat{a}_{T\lambda}/\cos(\lambda - \gamma_T)$ as target maneuver estimation. However, it should be noted that when $\lambda - \gamma_T$ is close to $\pm\pi/2$, such estimation may suffer from the problem of singularity. With a simple modification by using the property of trigonometric function, estimation strategy (19) completely avoids the singular issue. Figure 2 presents the comparison results of these two different strategies, where the simulation conditions can be found in Sec. IV.

5.2. Sliding Surface Design. To begin with, let $\lambda_e(k) = \lambda(k) - \lambda_F(k)$ denote the LOS angle tracking error, then. Based on Euler discretization concept and Eq. (6), the discrete-time angle error dynamics can be obtained as

$$\begin{aligned} \lambda_e(k+1) &= \lambda_e(k) + T\dot{\lambda}_e(k) \\ \dot{\lambda}_e(k+1) &= \dot{\lambda}(k) - \frac{2T\dot{R}(k)\dot{\lambda}(k)}{R(k)} + \frac{Ta_{T\lambda}(k)}{R(k)} - \frac{Ta_{M\lambda}(k)}{R(k)} \\ &\quad - \dot{\lambda}_F(k) - \frac{\delta(k)}{V_T}. \end{aligned} \tag{20}$$

Let t_f and N be the final impact time and impact step, respectively. Then, the relationship between t_f and N can be obtained as $N = round(t_f/T)$, where $round(\cdot)$ denotes the round operator for $(\cdot)$ to obtain the nearest integer. Based on the concept of time-to-go, the final impact step N can be estimated as

$$N = round\left(t_f/T\right) = round\left(-R/\dot{R}\right) + k. \tag{21}$$

Next, consider the following time-varying sliding surface

$$s(k) = \dot{\lambda}_e(k) + f(k)\lambda_e(k), \tag{22}$$

where $f(k) = c/[(N-k)T]$ and $c > 0$ is a user-designed parameter. It can be noted that with the increasing of k, the convergence speed of the angle tracking error also increases. Generally, using $-R/\dot{R}$ to approximate time-to-go in (21) would generate smaller value during the initial flight phase,

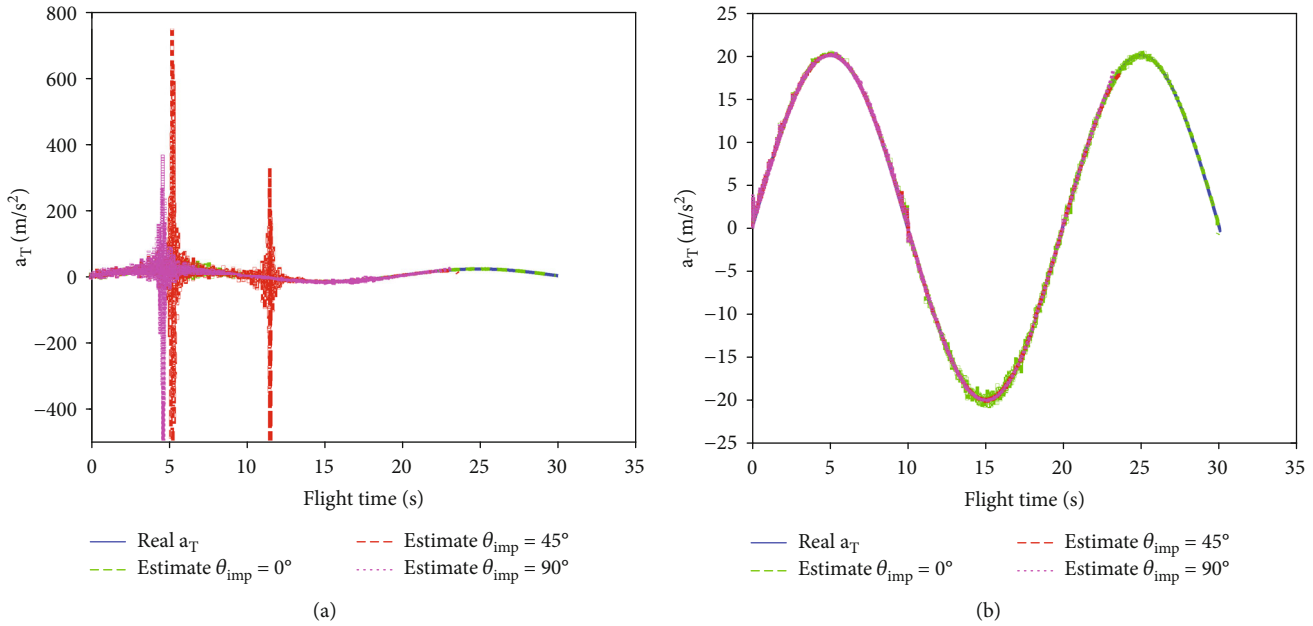

Figure 2: Comparison of two target maneuver estimation strategy: (a) estimation algorithm [27]; and (b) estimation algorithm (19).

but this approximation error will just speed up the convergence phase and not affect the angle tracking accuracy. The characteristics of sliding surface (22) are presented in the following theorem.

Theorem 2. *If the closed-loop system enters a small region around the sliding manifold, e.g., $|s(k)| \le \varepsilon$, both LOS angle tracking error and its rate will be bounded by some small positive constants.*

Proof. Using Euler discretization approach, one can obtain that

$$|s(k)| = \left|\frac{\lambda_e(k+1) - \lambda_e(k)}{T} + f(k)\lambda_e(k)\right| \le \varepsilon. \tag{23}$$

Following the preceding equation, it can be deduced that

$$\begin{aligned}|\lambda_e(k+1)| &\le \left(1 - \frac{c}{N-k}\right)|\lambda_e(k)| + \varepsilon T \le \left(1 - \frac{1}{N-k}\right)^c |\lambda_e(k)| + \varepsilon T \\ &\le \left(1 - \frac{k}{N}\right)^c |\lambda_e(0)| + \underbrace{\varepsilon T \sum_{i=1}^{k} \left(1 - \frac{k-j}{N-i}\right)}_{\bar{M}}.\end{aligned} \tag{24}$$

Inequality (24) shows that $|\lambda_e(k+1)|$ is ultimately upper bounded by $\bar{M}$, and therefore, $\dot{\lambda}_e(k)$ is also upper bounded by $|\dot{\lambda}_e(k)| = |\lambda_e(k+1) - \lambda_e(k)|/T \le 2\bar{M}/T$. This completes the proof.

Theorem 2 shows that if the closed-loop system trajectory can be forced into a small region around the sliding surface, both the LOS angle tracking error and its rate can also be bounded by some small positive constants, leading to successful interception with impact angle constraint.

5.3. Guidance Law Design. For guidance law design, deriving the sliding manifold dynamics as

$$\begin{aligned}s(k+1) &= \dot{\lambda}_e(k+1) + f(k+1)\lambda_e(k+1) \\ &= \dot{\lambda}(k) - \frac{2T\dot{R}(k)\dot{\lambda}(k)}{R(k)} + \frac{Ta_{T\lambda}(k)}{R(k)} - \frac{Ta_{M\lambda}(k)}{R(k)} \\ &\quad - \dot{\lambda}_F(k) - \frac{\delta(k)}{V_T} + \frac{c}{(N-k-1)T}\lambda_e(k+1) \\ &= \dot{\lambda}(k) - \frac{2T\dot{R}(k)\dot{\lambda}(k)}{R(k)} + \frac{Ta_{T\lambda}(k)}{R(k)} - \frac{Ta_{M\lambda}(k)}{R(k)} \\ &\quad - \dot{\lambda}_F(k) - \frac{\delta(k)}{V_T} + \frac{c}{(N-k)(N-k-1)T}\lambda_e(k+1) \\ &\quad + \frac{c}{(N-k)T}\lambda_e(k+1) \\ &= s(k) - \frac{2T\dot{R}(k)\dot{\lambda}(k)}{R(k)} + \frac{Ta_{T\lambda}(k)}{R(k)} - \frac{Ta_{M\lambda}(k)}{R(k)} \\ &\quad - \frac{\delta(k)}{V_T} + \frac{f(k)}{N-k-1}\lambda_e(k) + \frac{Tf(k)}{N-k-1} \\ &\quad \left[\dot{\lambda}(k) - \frac{a_T(k)}{V_T}\right] + Tf(k)\left[\dot{\lambda}(k) - \frac{a_T(k)}{V_T}\right] \\ &= s(k) - \frac{2T\dot{R}(k)\dot{\lambda}(k)}{R(k)} + \frac{Ta_{T\lambda}(k)}{R(k)} - \frac{Ta_{M\lambda}(k)}{R(k)} - \frac{\delta(k)}{V_T} \\ &\quad + \frac{f(k)}{N-k-1}\lambda_e(k) + \frac{c}{N-k-1}\left[\dot{\lambda}(k) - \frac{a_T(k)}{V_T}\right].\end{aligned} \tag{25}$$

Table 1: Required data for initializing simulations.

Parameter	Value
Initial relative range	$R(0) = \boldsymbol{10000m}$
Initial flight path angle	$\gamma_M(0) = \pi/4\boldsymbol{rad}$, $\gamma_T(0) = \pi\boldsymbol{rad}$
Initial LOS angle	$\lambda(0) = \pi/6\boldsymbol{rad}$
Flying velocity	$V_M = \boldsymbol{400m/s}$, $V_T = \boldsymbol{200m/s}$
Target maneuver	Case 1: $a_T = 20\boldsymbol{m/s^2}$ Case 2: $a_T = 20\sin(0.1t)\boldsymbol{m/s^2}$

Table 2: Mean miss distances and impact angle errors of 50 runs Monte-Carlo simulations.

		$\theta_{imp} = 0^\circ$	$\theta_{imp} = 45^\circ$	$\theta_{imp} = 90^\circ$
Case 1	Miss distance	0.749 m	0.659 m	0.713 m
	Impact angle error	0.455 deg	0.391 deg	0.317 deg
Case 2	Miss distance	0.758 m	0.788 m	0.695 m
	Impact angle error	0.501 deg	0.389 deg	0.426 deg

For sliding variable dynamics (25), the proposed super-twisting-like guidance law is defined as

$$\begin{aligned} a_{M\lambda}(k) &= -2\dot{R}(k)\dot{\lambda}(k) + \widehat{a}_{T\lambda}(k) + \frac{f(k)R(k)\lambda_e(k)}{(N-k-1)T} \\ &\quad + \frac{cR(k)\dot{\lambda}(k)}{(N-k-1)T} - \frac{cR(k)\widehat{a}_T(k)}{(N-k-1)TV_T} + \frac{\rho_1 R(k)s(k)}{T} \\ &\quad - R(k)\xi(k) + k_1 R(k)\boldsymbol{sig}^{0.5}(s(k))\xi(k+1) \\ &= \rho_2\xi(k) - Tk_2\boldsymbol{sgn}(s(k)), \end{aligned} \tag{26}$$

where $0 < \rho_1 < 1$, $0 < \rho_2 < 1$, $k_1 > 0$, and $k_2 > 0$, $\boldsymbol{sig}^{0.5}(s(k)) = \mathrm{sgn}(s(k))|s(k)|^{0.5}$ is a nonsmooth but continuous function.

It follows from Eq. (26) that the key features of the proposed guidance law are two folds. The first one lies in its chattering-mitigation property due to the fact that $\boldsymbol{sig}^{0.5}(\cdot)$ in guidance command (26) is a nonsmooth but continuous function, and the second one is that the presented guidance law requires no information on target maneuvers by using a model-assisted discrete-time disturbance observer.

Theorem 3. *For discrete-time sliding mode dynamics (25) under Assumptions 1-5, if the guidance law is designed as (26) with target maneuver estimation (12), (19), then the system trajectory can be forced to enter a small region around the sliding surface, and therefore, precise interception with impact angle constraint is ensured.*

Proof. Substituting guidance law (26) into (25) yields

$$s(k+1) = (1-\rho_1)s(k) + T\xi(k) - Tk_1\boldsymbol{sig}^{0.5}(s(k)) + T\Delta(k), \tag{27}$$

$$\xi(k+1) = \rho_2\xi(k) - Tk_2\boldsymbol{sgn}(s(k)), \tag{28}$$

where $\Delta(k) = (a_{T\lambda} - \widehat{a}_{T\lambda})/R(k) - c(a_T - \widehat{a}_T)/[(N-k-1)TV_T] - \delta(k)/(TV_T)$. For convenience of analysis, defining $\bar{\rho}_1 = 1 - \rho_1 \in (0,1)$, $\zeta(k) = \xi(k) + \delta(k)$, then system (28) can be rewritten as

$$s(k+1) = \bar{\rho}_1 s(k) + T\zeta(k) - Tk_1\boldsymbol{sig}^{0.5}(s(k)), \tag{29}$$

$$\zeta(k+1) = \rho_2\zeta(k) - Tk_2\boldsymbol{sgn}(s(k)) + T\eta(k), \tag{30}$$

where $\eta(k) = (1-\rho_2)\Delta(k)/T$. For a realistic interception, the missile-target relative range is always bounded. With this in mind and considering Theorem 1 as well as Assumption 5, one can imply that $\eta(k)$ is also upper bounded, i.e., $|\eta(k)| \le \eta^*$ with η^* being a positive constant.

Let $\boldsymbol{x}(k) = [s(k), \zeta(k)]^T$, then, system (30) can be represented as the following matrix form

$$\boldsymbol{x}(k+1) = \boldsymbol{A}\boldsymbol{x}(k) + \boldsymbol{B}(k)\mathtt{sign}(s(k)), \tag{31}$$

where $\boldsymbol{A} \in \mathbb{R}^{2\times 2}$ and $\boldsymbol{B}(k) \in \mathbb{R}^2$ are defined as

$$\boldsymbol{A} = \begin{bmatrix} \bar{\rho}_1 & T \\ 0 & \rho_2 \end{bmatrix}, \quad \boldsymbol{B}(k) = \begin{bmatrix} -Tk_1\mathtt{sig}^{0.5}(s(k)) \\ -Tk_2\mathtt{sgn}(s(k)) + T\eta(k) \end{bmatrix}. \tag{32}$$

Suppose that the gains ρ_1 and ρ_2 are properly chosen such that the following discrete-time Lyapunov equation

$$\boldsymbol{A}^T(\boldsymbol{P} + \boldsymbol{P}\boldsymbol{\Lambda}\boldsymbol{P})\boldsymbol{A} - (1-\ell)\boldsymbol{P} + \boldsymbol{Q} \le 0, \tag{33}$$

with $0 < \ell < 1$, has a positive-definite solution $\boldsymbol{P} = \boldsymbol{P}^T > 0$ for a given $\boldsymbol{Q} = \boldsymbol{Q}^T > 0$ and $\boldsymbol{\Lambda} = \boldsymbol{\Lambda}^T > 0$.

For system (31), consider $V(k) = \boldsymbol{x}^T(k)\boldsymbol{P}\boldsymbol{x}(k)$ as a Lyapunov function candidate, then one has

$$\Delta V(k) = V(k+1) - V(k) = \boldsymbol{x}^T(k+1)\boldsymbol{P}\boldsymbol{x}(k+1) - \boldsymbol{x}^T(k)\boldsymbol{P}\boldsymbol{x}(k). \tag{34}$$

Substituting Eq. (31) into (34) yields

$$\begin{aligned} \Delta V(k) &= \boldsymbol{x}^T(k)\left(\boldsymbol{A}^T\boldsymbol{P}\boldsymbol{A} - \boldsymbol{P}\right)\boldsymbol{x}(k) \\ &\quad + 2\boldsymbol{x}^T(k)\boldsymbol{A}^T\boldsymbol{P}\boldsymbol{B}(k)\mathtt{sign}(V_\lambda(k)) \\ &\quad + \boldsymbol{B}^T(k)\boldsymbol{P}\boldsymbol{B}(k). \end{aligned} \tag{35}$$

Applying lambda inequality $\boldsymbol{X}^T\boldsymbol{Y} + \boldsymbol{Y}^T\boldsymbol{X} \le \boldsymbol{X}^T\boldsymbol{\Lambda}^{-1}\boldsymbol{X} + \boldsymbol{Y}^T\boldsymbol{\Lambda}\boldsymbol{Y}$, one has

$$2\boldsymbol{x}^T(k)\boldsymbol{A}^T\boldsymbol{P}\boldsymbol{B}(k)\mathtt{sign}(V_\lambda(k)) \le \boldsymbol{x}^T(k)\boldsymbol{A}^T\boldsymbol{P}\boldsymbol{\Lambda}\boldsymbol{P}\boldsymbol{A}\boldsymbol{x}(k) + \boldsymbol{B}^T(k)\boldsymbol{\Lambda}^{-1}\boldsymbol{B}(k). \tag{36}$$

Substituting inequality (36) into (35) gives

$$\begin{aligned}\Delta V(k) &\le \boldsymbol{x}^T(k)\left[\boldsymbol{A}^T(\boldsymbol{P}+\boldsymbol{P}\boldsymbol{\Lambda}\boldsymbol{P})\boldsymbol{A}-(1-\ell)\boldsymbol{P}\right]\boldsymbol{x}(k)\\ &\quad+\boldsymbol{B}^T(k)\left(\boldsymbol{\Lambda}^{-1}+\boldsymbol{P}\right)\boldsymbol{B}(k)-\ell V(k)\\ &\le \boldsymbol{x}^T(k)\boldsymbol{Q}\boldsymbol{x}(k)+\boldsymbol{B}^T(k)\boldsymbol{Z}\boldsymbol{B}(k)-\ell V(k),\end{aligned} \tag{37}$$

where $\boldsymbol{Z}=\boldsymbol{\Lambda}^{-1}+\boldsymbol{P}$. Expanding the term $\boldsymbol{B}^T(k)\boldsymbol{Z}\boldsymbol{B}(k)$ leads to

$$\boldsymbol{B}^T(k)\boldsymbol{Z}\boldsymbol{B}(k)=\delta_1|s(k)|+\delta_2|s(k)|^{1/2}+\delta_3, \tag{38}$$

$$\delta_1=z_{11}k_1^2T^2,\quad \delta_2=2z_{12}k_1k_2T^2-2z_{12}k_1T^2\eta(k), \tag{39}$$

$$\delta_3=z_{22}k_2^2T^2+z_{22}T^2\eta^2(k)-2z_{22}T^2k_2\eta(k)\ \mathrm{sgn}\ (s(k)). \tag{40}$$

Note that $\forall x\in\mathbb{R}$, $0<\rho<1$, the inequality $|x|^\rho<1+|x|$ holds. Then, it follows from Eq. (38) that

$$\boldsymbol{B}^T(k)\boldsymbol{Z}\boldsymbol{B}(k)\le(\delta_1+\delta_2)|s(k)|+\delta_2+\delta_3. \tag{41}$$

By choosing $\bar{k}_2=k_2-\eta^*>0$, inequality (41) can be further reduced to

$$\begin{aligned}&\boldsymbol{B}^T(k)\boldsymbol{Z}\boldsymbol{B}(k)\le\bar{\delta}_1|s(k)|+\bar{\delta}_2,\\ &\bar{\delta}_1=\delta_1+2z_{12}k_1\bar{k}_2T^2,\quad \bar{\delta}_2=2z_{12}k_1\bar{k}_2T^2+z_{22}T^2\left(k_2^2+(\eta^*)^2+2k_2\eta^*\right).\end{aligned} \tag{42}$$

Following the previous result, one can imply that

$$\begin{aligned}\Delta V(k)&\le\boldsymbol{x}^T(k)\boldsymbol{Q}\boldsymbol{x}(k)+\bar{\delta}_1|s(k)|+\bar{\delta}_2-\ell V(k)\\ &\le\boldsymbol{x}^T(k)\boldsymbol{Q}\boldsymbol{x}(k)+\bar{\delta}_1\|\boldsymbol{x}(k)\|+\bar{\delta}_2-\ell V(k)\\ &\le\boldsymbol{x}^T(k)\boldsymbol{Q}\boldsymbol{x}(k)+\bar{\delta}_1\left\|\boldsymbol{Q}\boldsymbol{Q}^{-1}\boldsymbol{x}(k)\right\|+\bar{\delta}_2-\ell V(k)\\ &\le\boldsymbol{x}^T(k)\boldsymbol{Q}\boldsymbol{x}(k)+\bar{\delta}_1\left\|\boldsymbol{Q}\boldsymbol{Q}^{-1}\boldsymbol{x}(k)\right\|+\bar{\delta}_2-\ell V(k)\\ &\le-\left(\left\|\boldsymbol{Q}^{1/2}\boldsymbol{x}(k)\right\|-\frac{1}{2}\bar{\delta}_1\left\|\boldsymbol{Q}^{-1}\right\|\right)^T\left(\left\|\boldsymbol{Q}^{1/2}\boldsymbol{x}(k)\right\|-\frac{1}{2}\bar{\delta}_1\left\|\boldsymbol{Q}^{-1}\right\|\right)\\ &\quad+\bar{\delta}_2-\ell V(k)+\frac{1}{4}\bar{\delta}_1^2\left\|\boldsymbol{Q}^{-1}\right\|^2\\ &\le-\ell V(k)+c,\end{aligned} \tag{43}$$

where $c=\bar{\delta}_2+1/4\bar{\delta}_1^2\|\boldsymbol{Q}^{-1}\|^2$. Then,

$$V(k+1)\le(1-\ell)V(k)+c. \tag{44}$$

Solving inequality (44) yields

$$V(k+1)\le(1-\ell)^kV(0)+c\sum_{i=1}^{k}(1-\ell)^i. \tag{45}$$

If the upper limit when k goes to infinity is considered, one can conclude that

$$\lim_{k\to\infty}V(k)\le c/\ell. \tag{46}$$

Inequality (46) shows that the sliding variable $s(k)$ is upper bounded by $\sqrt{c/\ell}$, which also implies that the LOS tracking error and its rate are also upper bounded by small constants, and therefore, accurate interception with impact angle is satisfied. This completes the proof.

6. Simulation Studies

In this section, the effectiveness of the proposed guidance law is demonstrated through numerical simulations, in which a surface-to-air missile is considered to intercept a maneuvering head-on target during its terminal guidance phase.

6.1. Simulation Setup. The simulations are performed in Matlab/Simulink platform with a sampling rate 0.01 s. Here, the missile is supposed to be equipped with an active radar seeker, providing LOS angle, LOS angular rate, range, and range rate measurement. The required simulation data for Eqs. (1)–(4) are summarized in Table 1. Since the undesirable noise always exists in seeker measurement and will affect the performance of the closed-loop guidance system, simulations are performed in a noise-corrupted homing environment to approximate the practical engineering for the most.

6.2. Simulation Results for Different Impact Angles. The desired impact angles are set as $\theta_{imp}=0^\circ, 45^\circ, 90^\circ$ for both Cases 1 and 2. The mean miss distances and impact angle errors for these two cases with 50 runs Monte-Carlo simulations are summarized in Table 2. The simulation results, including interception trajectory, achieved acceleration, LOS angle profile, target maneuver projection estimation performance, impact angle profile as well as target maneuver estimation for Cases 1 and 2 are provided in Figures 3 and 4, where Figure 3 is for Case 1 and Figure 4 is for Case 2. The desired values for LOS angle in these figures are calculated using Eq. (10).

One can note from these two figures that accurate interception is achieved under the proposed guidance law whatever the desired impact angle is, that is, the miss distances in these scenarios are less than $0.8\boldsymbol{m}$. These figures also demonstrate that the LOS angles converge to their corresponding desired values during the homing engagement and therefore proves that the proposed guidance law exhibits satisfactory performance in impact angle control with the small acceptable miss distance for different impact angles, that is, the impact angle errors in these scenarios are less than 0.5 deg. These results also show that the proposed model-assisted discrete-time disturbance observer can accurately track the real target maneuver in noise-corrupted guidance environment.

6.3. Comparison Results with Existing Discrete-Time Sliding Mode Guidance Law. To illustrate the effectiveness of the proposed guidance law, the existing discrete-time sliding mode control guidance (DSMCG) law [30] is also performed in simulations in this subsection for the purpose of comparison. In view of the idea of classical DSMC, the DSMCG law is formulated as

$$a_M(k)=-2\dot{R}(k)\dot{\lambda}(k)+\beta\boldsymbol{sgn}\left(\dot{\lambda}(k)\right), \tag{47}$$

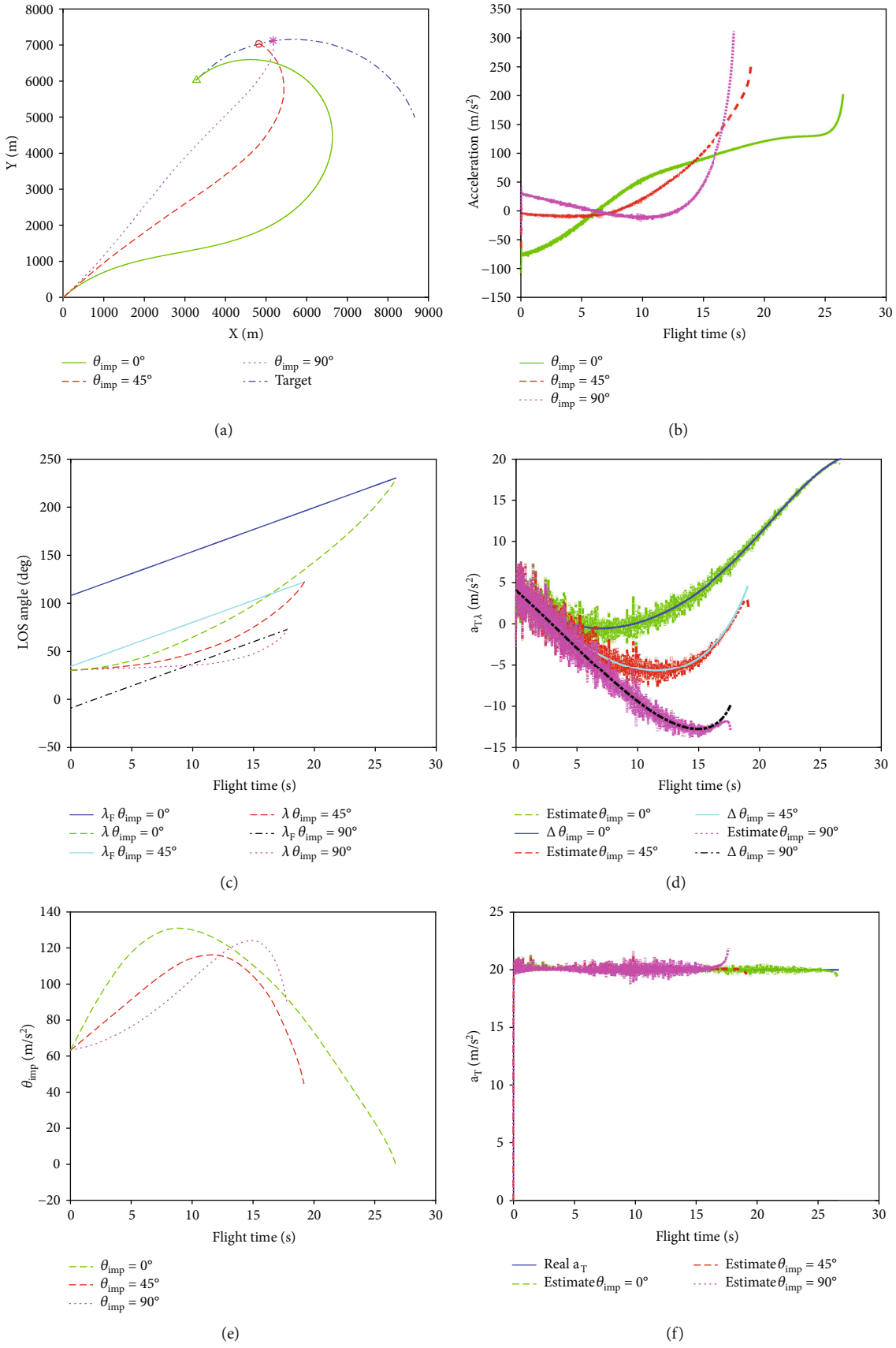

Figure 3: Simulation results under the proposed guidance law for Case 1: (a) interception trajectory; (b) missile achieved acceleration; (c) LOS angle profile; (d) target maneuver projection estimation; (e) impact angle profile; and (f) target maneuver estimation.

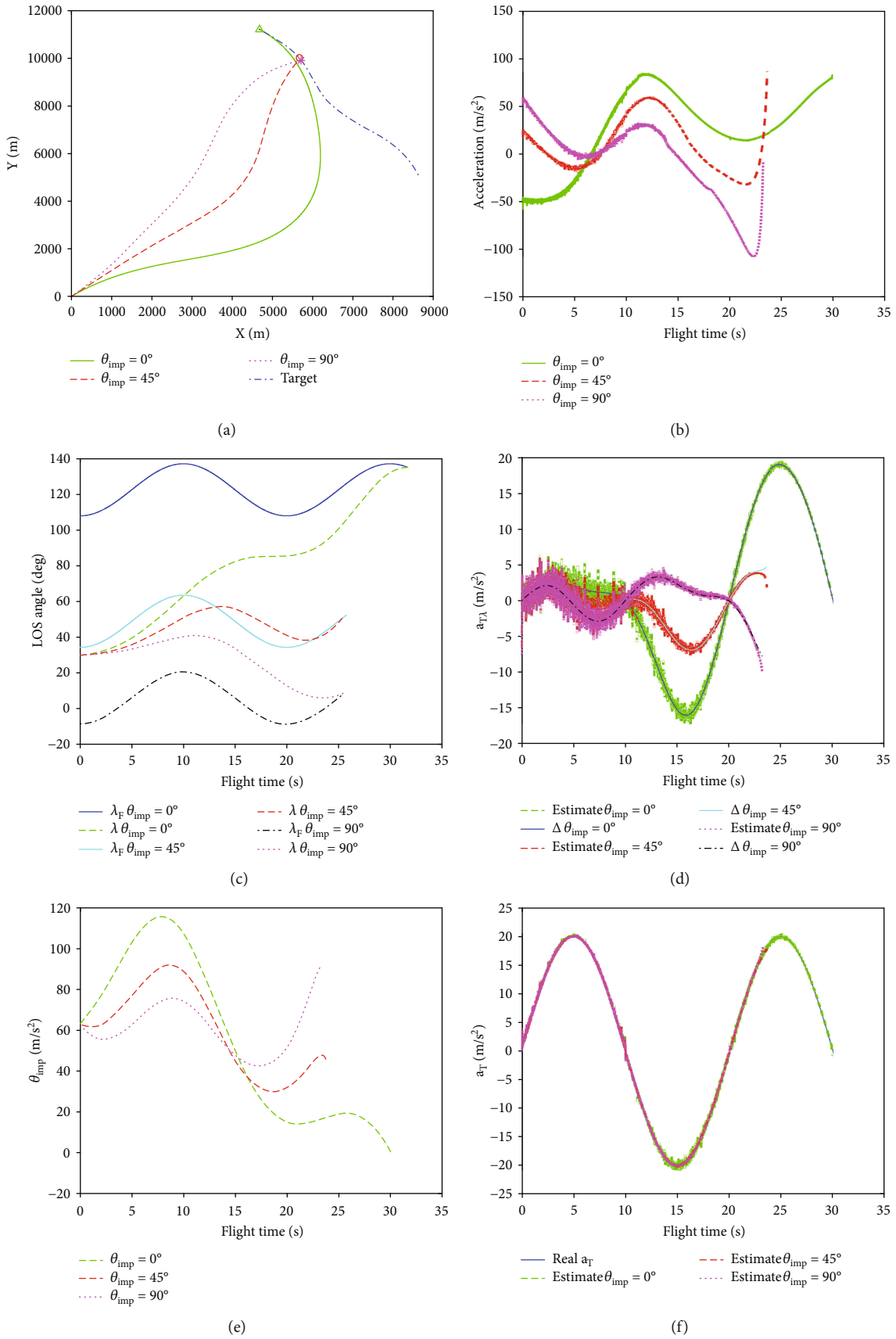

Figure 4: Simulation results under the proposed guidance law for Case 2: (a) interception trajectory; (b) missile achieved acceleration; (c) LOS angle profile; (d) target maneuver projection estimation; (e) impact angle profile; and (f) target maneuver estimation.

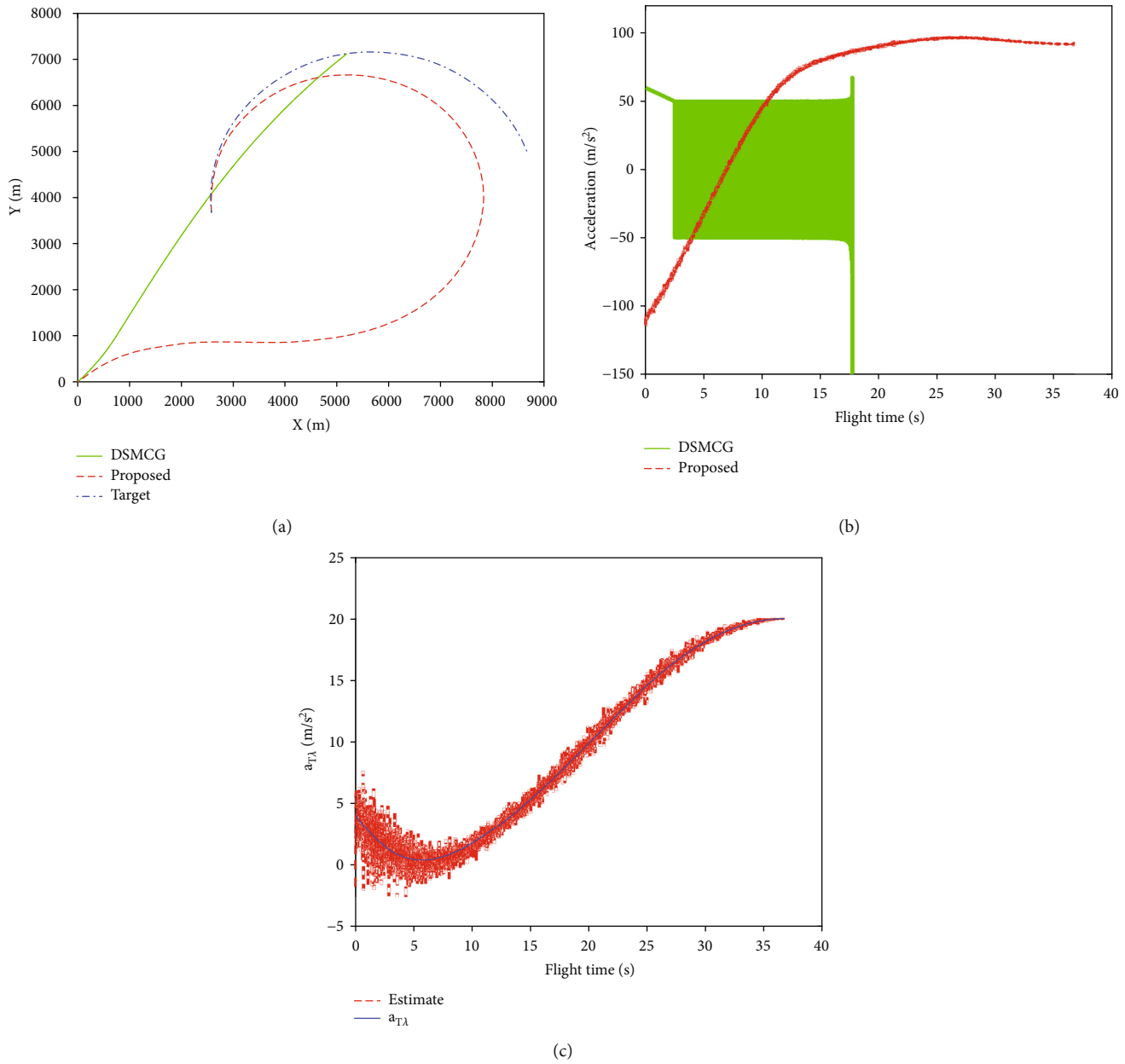

FIGURE 5: Simulation results under the proposed guidance law for Case 1: (a) interception trajectory; (b) achieved acceleration; and (c) target maneuver estimation.

where $\beta > 0$ is the guidance gain to be designed. To effectively counteract the effect of target maneuver, the guidance gain β needs to be larger than the maximum magnitude of target maneuver. It can be noted that the discontinuous function $\boldsymbol{sgn}(\dot{\lambda}(k))$ would result in high-frequency chattering in real applications.

The simulation results, including interception trajectory, achieved acceleration, target maneuver estimation performance, with $\theta_{imp} = 0^{\circ}$ for Cases 1 and 2 are shown in Figures 5 and 6, which clearly demonstrate the chattering-mitigation property of the proposed guidance law. Moreover, as the main concern of DSMCG law is to nullify the LOS rate, this guidance law cannot be used for impact angle control. It should be noted that implementing the DMSCG law requires the information on the upper bound of target maneuver to choose the switching gain. However, such assumption on the knowledge of the upper bound of target maneuver would result in a design dilemma as discussed in Sec. I. As a comparison, the proposed guidance law adopts a disturbance observer to estimate the target maneuver, and therefore, it requires no priori knowledge on target maneuvers, bringing some advantages for practical implementation.

7. Conclusions

Under the framework of sliding mode control, the problem of intercepting unknown maneuvering targets with impact angle constraint is investigated by a new discrete-

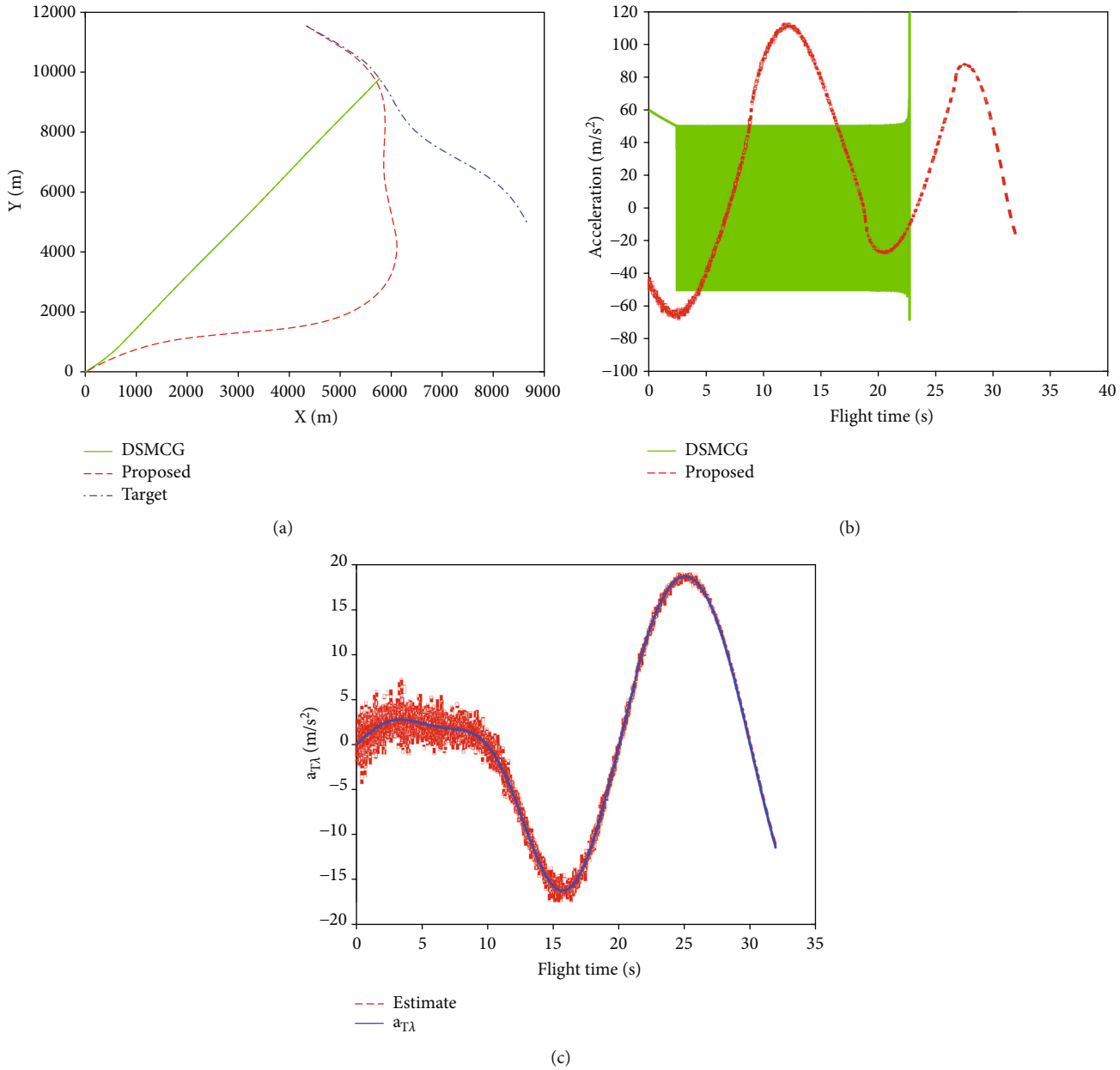

FIGURE 6: Simulation results under the proposed guidance law for Case 2: (a) interception trajectory; (b) achieved acceleration; and (c) target maneuver estimation.

time guidance law enhanced by a disturbance observer. A model-assisted discrete-time disturbance observer is first proposed to estimate the target maneuver, and theoretical analysis shows that the estimation error is exponentially stable with a small upper bound determined by the sampling rate. Based on the reconstructed target maneuver information, a chattering-mitigated super-twisting-like discrete-time guidance law is proposed to force the system trajectory to converge into a small region around the sliding surface, and therefore, accurate interception with impact angle constraint is satisfied. Simulation and comparison studies of a surface-to-air missile have been carried out to show the efficiency of the proposed approach.

Data Availability

The data used to support the findings of this study are included within the article.

Conflicts of Interest

The authors declare that there is no conflict of interest regarding the publication of this paper.

Acknowledgments

This work was supported by the National Natural Science Foundation of China under grant U1613225.

References

[1] P. Zarchan, *Tactical and Strategic Missile Guidance*, AIAA, Reston, VA, 1997.

[2] S. He and C. Lee, "Optimal proportional-integral guidance with reduced sensitivity to target maneuvers," *IEEE Transactions on Aerospace and Electronic Systems*, vol. 54, no. 5, pp. 2568–2579, 2018.

[3] S. He and C. H. Lee, "Optimality of error dynamics in missile guidance problems," *Journal of Guidance, Control, and Dynamics*, vol. 41, no. 7, pp. 1624–1633, 2018.

[4] S. He, T. Song, and D. Lin, "Impact angle constrained integrated guidance and control for maneuvering target interception," *Journal of Guidance, Control, and Dynamics*, vol. 40, no. 10, pp. 2653–2661, 2017.

[5] Y.-I. Lee, S.-H. Kim, J.-I. Lee, and M.-J. Tahk, "Analytic solutions of generalized impact-angle-control guidance law for first-order lag system," *Journal of Guidance, Control, and Dynamics*, vol. 36, no. 1, pp. 96–112, 2013.

[6] C. K. Ryoo, H. Cho, and M. J. Tahk, "Optimal guidance laws with terminal impact angle constraint," *Journal of Guidance, Control, and Dynamics*, vol. 28, no. 4, pp. 724–732, 2005.

[7] C.-K. Ryoo, H. Cho, and M.-J. Tahk, "Time-to-go weighted optimal guidance with impact angle constraints," *IEEE Transactions on Control Systems Technology*, vol. 14, no. 3, pp. 483–492, 2006.

[8] E. J. Ohlmeyer and C. A. Phillips, "Generalized vector explicit guidance," *Journal of Guidance, Control, and Dynamics*, vol. 29, no. 2, pp. 261–268, 2006.

[9] H. Cho, C. K. Ryoo, A. Tsourdos, and B. White, "Optimal impact angle control guidance law based on linearization about collision triangle," *Journal of Guidance, Control, and Dynamics*, vol. 37, no. 3, pp. 958–964, 2014.

[10] D. E. Kirk, *Optimal Control Theory: An Introduction*, Prentice-Hall, New York, NY, 1970.

[11] T. Shima, "Intercept-angle guidance," *Journal of Guidance, Control, and Dynamics*, vol. 34, no. 2, pp. 484–492, 2011.

[12] S. Rao and D. Ghose, "Terminal impact angle constrained guidance laws using variable structure systems theory," *IEEE Transactions on Control Systems Technology*, vol. 21, no. 6, pp. 2350–2359, 2013.

[13] S. R. Kumar, S. Rao, and D. Ghose, "Sliding-mode guidance and control for all-aspect interceptors with terminal angle constraints," *Journal of Guidance, Control, and Dynamics*, vol. 35, no. 4, pp. 1230–1246, 2012.

[14] S. R. Kumar, S. Rao, and D. Ghose, "Nonsingular terminal sliding mode guidance with impact angle constraints," *Journal of Guidance, Control, and Dynamics*, vol. 37, no. 4, pp. 1114–1130, 2014.

[15] Q. Li, G. Han, W. Zhang, and Y. Yang, "Adaptive neuro-fuzzy sliding mode control guidance law with impact angle constraint," *IET Control Theory & Applications*, vol. 9, no. 14, pp. 2115–2123, 2015.

[16] S. He, D. Lin, and J. Wang, "Robust terminal angle constraint guidance law with autopilot lag for intercepting maneuvering targets," *Nonlinear Dynamics*, vol. 81, no. 1-2, pp. 881–892, 2015.

[17] S. He, D. Lin, and J. Wang, "Continuous second-order sliding mode based impact angle guidance law," *Aerospace Science and Technology*, vol. 41, pp. 199–208, 2005.

[18] Z. Zhu, D. Xu, J. Liu, and Y. Xia, "Missile guidance law based on extended state observer," *IEEE Transactions on Industrial Electronics*, vol. 12, no. 60, pp. 5882–5891, 2013.

[19] S. E. Talole, A. Ghosh, and S. B. Phadke, "Proportional navigation guidance using predictive and time delay control," *Control Engineering Practice*, vol. 14, no. 12, pp. 1445–1453, 2006.

[20] Y. B. Shtessel, I. A. Shkolnikov, and A. Levant, "Smooth second- order sliding modes: missile guidance application," *Automatica*, vol. 43, no. 8, pp. 1470–1476, 2007.

[21] S. B. Phadke and S. E. Talole, "Sliding mode and inertial delay control based missile guidance," *IEEE Transactions on Aerospace and Electronic Systems*, vol. 4, pp. 3331–3346, 2012.

[22] S. He, J. Wang, and D. Lin, "Composite guidance Laws using higher order sliding mode differentiator and disturbance observer," *Proceedings of the Institution of Mechanical Engineers, Part G: Journal of Aerospace Engineering*, vol. 229, no. 13, pp. 2397–2415, 2015.

[23] Y. P. Lin, C. L. Lin, P. Suebsaiprom, and S. L. Hsieh, "Estimating evasive acceleration for ballistic targets using an extended state observer," *IEEE Transactions on Aerospace and Electronic Systems*, vol. 52, no. 1, pp. 337–349, 2016.

[24] A. Argha, S. Su, L. Li, H. T. Nguyen, and B. G. Celler, *Advances in Discrete-Time Sliding Mode Control: Theory and Applications*, CRC Press, 2018.

[25] S. Janardhanan and B. Bandyopadhyay, "Discrete sliding mode control of systems with unmatched uncertainty using multirate output feedback," *IEEE Transactions on Automatic Control*, vol. 51, no. 6, pp. 1030–1035, 2006.

[26] S. He, W. Wang, and J. Wang, "Discrete-Time Super-Twisting Guidance Law with Actuator Faults Consideration," *Asian Journal of Control*, vol. 19, pp. 1854–1861, 2017.

[27] R. W. Morgan, H. Tharp, and T. L. Vincent, "Minimum energy guidance for aerodynamically controlled missiles," *IEEE Transactions on Automatic Control*, vol. 56, no. 9, pp. 2026–2037, 2011.

[28] A. G. Rawling, "On nonzero miss distance," *Journal of Spacecraft and Rockets*, vol. 6, no. 1, pp. 81–83, 1969.

[29] S. Xiong, W. Wang, X. Liu, S. Wang, and Z. Chen, "Guidance law against maneuvering targets with intercept angle constraint," *ISA Transactions*, vol. 53, no. 4, pp. 1332–1342, 2014.

[30] D. Zhou, S. Sun, J. Y. Zhou, and K. L. Teo, "A discrete sliding-mode guidance law," *Journal of Dynamic Systems, Measurement, and Control*, vol. 137, no. 2, 2015.